

Strong and Noise-Tolerant Entanglement in Dissipative Optomechanics

Jiaojiao Chen,¹ Wei Xiong,^{2,3,*} Dong Wang,¹ and Liu Ye^{1,†}

¹*Department of Physics and Optoelectronic Engineering, Anhui University, Anhui 230000, China*

²*Department of Physics, Wenzhou University, Zhejiang, 325035, China*

³*International Quantum Academy, Shenzhen, 518048, China*

(Dated: January 17, 2025)

Macroscopic entanglement, as critical quantum resources in quantum information science, has been extensively studied in optomechanical systems with purely dispersive coupling over the past decades. However, quantum entanglement, induced by *purely dissipative coupling*, remains unexplored. In this work, we study quantum entanglement in a Michelson–Sagnac interferometer, where the dispersive and the dissipative coupling can be *arbitrarily switched on and off*. With current experimental parameters, we demonstrate that the steady-state mechanical displacement exhibits a nonlinear (linear) dependence on the driving power with the purely dispersive (dissipative) coupling. Further, we find that quantum entanglement generated by purely dissipative coupling is significantly stronger and more noise-tolerant than that generated by purely dispersive coupling. When both couplings coexist, entanglement is weakened due to interference. Our findings provide a promising path to engineer strong and noise-tolerant quantum entanglement in purely dissipative quantum systems.

I. INTRODUCTION

Due to its potential applications in gravitational wave detection [1] and quantum-classical boundary tests [2], cavity optomechanics has garnered significant theoretical and experimental interest in quantum information science [3]. With advances in ground-state cooling [4–7], exploring quantum effects in cavity optomechanics has become a reality [8–27], especially for macroscopic quantum entanglement [28]. Over the past two decades, numerous theoretical proposals have been put forward to achieve optomechanical entanglement [29–38]. Experimentally, macroscopic entanglement between two massive oscillators has also been realized in cavity optomechanics experimentally [39]. Notably, both theoretical and experimental proposals have predominantly relied on coherent dispersive coupling mechanisms between the cavity mode and the mechanical mode.

Very recently, unconventional *dissipative optomechanics* was first theoretically proposed in a superconducting microwave circuit [40] and later extended to a Michelson–Sagnac interferometers (MSI) with a movable membrane [41]. In such dissipative optomechanics, the cavity linewidth depends on the mechanical displacement [40], giving rise to the dissipative coupling between the mechanical and cavity modes. This unique coupling mechanism opens a potential avenue to investigate intriguing quantum phenomena, such as unconventional bistability [42], quantum squeezing [43], enhanced ground-state cooling [44, 45], quantum sensing [46], negative-damping instability [40], self-sustained oscillations [47], and phonon lasing [48, 49]. Experimentally, dissipative optomechanics have been demonstrated in various plat-

forms, including the MSI [50, 51], microdisc resonator coupled to a nanomechanical waveguide [52], photonic crystal split-beam nanocavity [53], graphene drums coupled to high-Q microsphere [54], and levitated sphere trapped by dual-beam optical tweezers [48]. It is evident that dissipative optomechanics has made significant progress both theoretically and experimentally. However, how dissipative optomechanics influences quantum entanglement, particularly under dissipative coupling or purely dissipative coupling conditions, remains an open and unexplored question.

In this work, we propose to investigate quantum entanglement in an experimentally feasible dissipative optomechanical system [50, 51]. The setup consists of a fixed perfect mirror and an effective movable mirror, realized by a Michelson–Sagnac interferometer (MSI) incorporating a membrane. Compared to dispersive optomechanics [28] with negligible dissipative coupling, the dispersive and dissipative couplings can be independently *switched on and off* by adjusting the membrane position or the reflectivity (transmissivity) of the beam splitter (BS) in this unconventional dissipative optomechanics [41]. We first examine the behavior of the steady-state mechanical displacement with purely dispersive or dissipative coupling. It is evident that the displacement exhibits nonlinear dependence on the driving power with purely dispersive coupling, similar to conventional optomechanical systems [3]. However, it becomes linear dependence of the driving power for purely dissipative coupling. We then study the effect of the purely dispersive or dissipative coupling on generation of quantum entanglement. We surprisingly find that the quantum entanglement induced by purely dissipative coupling is not only much stronger than that generated by purely dispersive coupling, but also it is more robust against the bath temperature. For purely dispersive entanglement, its survival temperature is approximately ~ 8.5 K, while for purely dissipative entanglement, it can be up to ~ 25 K.

*xiongweiphys@wzu.edu.cn

†yeliu@ahu.edu.cn

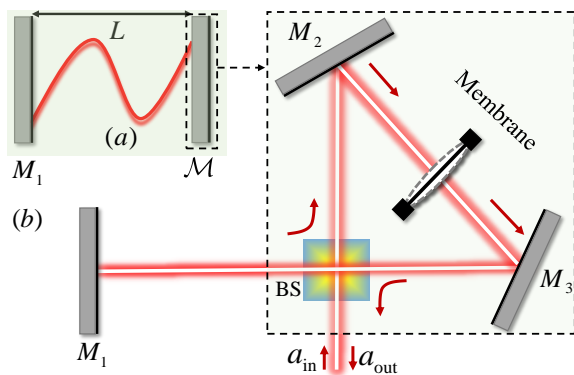


FIG. 1: (a) Schematic diagram of a typical dissipative optomechanical system, realized by a perfect fixed mirror M_1 and an effective movable mirror \mathcal{M} . (b) The structure of the effective movable mirror \mathcal{M} . The effective mirror consists of a Michelson-Sagnac interferometer (made up of a beam-splitter and two mirrors M_2 and M_3) and a movable membrane (mechanical resonator). L is the effective length of the cavity ($2L$ is the length of the Sagnac mode $M_1 - \text{BS} - M_2 - M_3 - \text{BS}$). a_{in} is the input port and a_{out} is the output port.

When both couplings coexist, entanglement reduces due to quantum interference. Our work provides a promising path to generate strong and noise-resilient quantum entanglement in quantum systems with *purely dissipative coupling*.

This paper is organized as follows. In Sec. II, we introduce the proposed model and its Hamiltonian. Then, the steady-state solutions of the system are investigated in Sec. III. In Sec. IV, the dynamics of the fluctuation and covariance matrix are given. In Secs. V, quantum entanglement is investigated. Finally, a conclusion is given in Sec. VI.

II. THE MODEL AND HAMILTONIAN

As shown in Fig. 1(a), we consider an experimentally feasible dissipative optomechanics [50, 51], consisting of a fixed mirror M_1 and an effective movable mirror \mathcal{M} . The effective mirror can be realized by a Michelson-Sagnac interferometer (MSI) and a movable membrane between mirrors M_2 and M_3 [see Fig. 1(b)]. L is the effective length of the cavity ($2L$ is the length of the Sagnac mode $M_1 - \text{BS} - M_2 - M_3 - \text{BS}$). The membrane is treated quantum mechanically, with its displacement and momentum operators denoted by x and p , respectively, satisfying the commutation relation $[x, p] = i\hbar$. Upon the introduction of an external driving field (with frequency ω_d and power P) at the beam splitter, the system can be effectively modeled as a typical dissipative optomechanical system. Thus, both the cavity frequency $\omega_a(x)$ and the decay rate $\kappa_a(x)$ depend on the displacement x of the membrane. For small membrane displacements x , we can Taylor expand $\omega_a(x)$ and $\kappa_a(x)$ to the first order, i.e., $\omega(x) \approx \omega_a - g_\omega x$ and $\kappa(x) \approx \kappa_a - g_\kappa x$, where ω_a

(κ_a) is the frequency (decay rate) of the cavity with annihilation (creation) operator a (a^\dagger) when the membrane is at its equilibrium. The Hamiltonian of the considered system is given by [40, 41]

$$H_S = (\omega_a - g_\omega x) a^\dagger a + \frac{1}{2} \omega_m (x^2 + p^2) + \int d\omega \omega a_\omega^\dagger a_\omega + ix' \int \frac{d\omega}{\sqrt{2\pi}} (a_\omega a^\dagger - a_\omega^\dagger a), \quad (1)$$

where ω_m is the frequency of the membrane, ω is the frequency of the bosonic mode (i.e., bath) with annihilation (creation) operator a_ω (a_ω^\dagger), $x' = \sqrt{2\kappa_a} - g_\kappa x / \sqrt{2\kappa_a}$ is the position-dependent coupling strength between the optical cavity and the bosonic mode. In fact, the bosonic mode here is to introduce a zero-value expectation input field $a_{\text{in}} = \int \frac{d\omega}{\sqrt{2\pi}} e^{-i\omega(t-t_0)} a_{\omega,0}$, with $a_{\omega,0}$ the operator at an initial time, to the cavity mode a , which can be easily obtained following the standard input-output theory with the Markov approximation. At the optical domain, the input field satisfies the relations [?]]

$$\begin{aligned} \langle a_{\text{in}}(t) a_{\text{in}}(t') \rangle &= 0, \\ \langle a_{\text{in}}(t) a_{\text{in}}^\dagger(t') \rangle &= \delta(t - t'). \end{aligned} \quad (2)$$

Substituting the input field a_{in} into Eq. (1), the Hamiltonian of the *driven* unconventional MSI, with respect to the driving frequency ω_d , becomes

$$\begin{aligned} \mathcal{H}_S &= (\Delta_a - g_\omega x) a^\dagger a + \frac{1}{2} \omega_m (x^2 + p^2) \\ &+ ix' (A_{\text{in}} a^\dagger - A_{\text{in}}^\dagger a), \end{aligned} \quad (3)$$

where $\Delta_a = \omega_a - \omega_d$ is the frequency detuning of the cavity mode from the driving field, and

$$A_{\text{in}} = a_{\text{in}} + \mathcal{E}. \quad (4)$$

Here $\mathcal{E} = |\mathcal{E}| \exp(i\theta)$, with $|\mathcal{E}| = \sqrt{\mathcal{P}/\hbar\omega_d}$ being the amplitude of the driving field and θ the phase. Notably, \mathcal{E} can also be interpreted as the steady-state value of the operator A_{in} , while a_{in} represents the fluctuation of A_{in} .

III. STEADY-STATE SOLUTION

When dissipation is included, the dynamics of the proposed system can be governed by the quantum Langevin equation $\mathcal{O} = -i[\mathcal{O}, \mathcal{H}_S] + \text{Dissipation} + \text{Noise}$, specifically,

$$\begin{aligned} \dot{x} &= \omega_m p, \\ \dot{p} &= g_\omega a^\dagger a - \omega_m x + \frac{ig_\kappa}{\sqrt{2\kappa_a}} (A_{\text{in}}^\dagger a - A_{\text{in}} a^\dagger) - \gamma_m p + \xi, \\ \dot{a} &= -(\kappa_a + i\Delta_a) a + ig_\omega a x + g_\kappa a x + x' A_{\text{in}}, \end{aligned} \quad (5)$$

where γ_m is the damping rate of the membrane and ξ is the Brownian noise operator arising from the coupling of the membrane oscillator to the hot environment. The correlation function of ξ is given by [56]

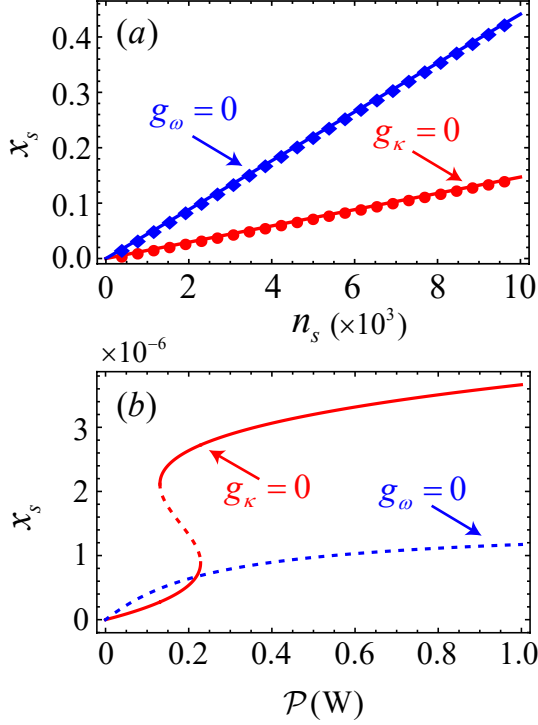


FIG. 2: The normalized steady-state displacement x_s of the membrane vs (a) the intracavity mean photon number $n_s = |a_s|^2$ and (b) the power of the driving field. The red curve corresponds to the case of the purely dispersive coupling ($g_\omega/2\pi = 2$ Hz). The blue curve is plotted for the purely dissipative coupling ($g_\kappa/2\pi = 2$ Hz). In (a) and (b), $\Delta_a = 3\kappa_a$ is assumed.

$\langle \xi(t)\xi(t') \rangle = \frac{\gamma_m}{\omega_m} \int \frac{d\omega}{2\pi} e^{-i\omega(t-t')} \omega [\coth(\frac{\hbar\omega}{2k_B T}) + 1]$. In the limit of the high quality factor, $\omega_m \gg \gamma_m$, the Brownian noise ξ becomes an approximate Markovian noise [57], i.e.,

$$\langle \xi(t)\xi(t') + \xi(t')\xi(t) \rangle / 2 \simeq \gamma_m (2n_{\text{th}} + 1) \delta(t - t') \quad (6)$$

where the mean thermal phonon number $n_{\text{th}} = [\exp(\hbar\omega_m/k_B T) - 1]^{-1}$ with k_B the Boltzmann constant and T the bath temperature.

When the evolution time is long enough, the system reaches its steady state, denoted by a_s , x_s , and p_s . From Eq. (5), the steady-state equation can be directly obtained as

$$\begin{aligned} \dot{x}_s &= \omega_m p_s, \\ \dot{p}_s &= g_\omega |a_s|^2 - \omega_m x_s + \frac{ig_\kappa}{\sqrt{2\kappa_a}} (\mathcal{E}^* a_s - \mathcal{E} a_s^*) - \gamma_m p_s, \\ \dot{a}_s &= -(\kappa_s + i\Delta_s) a_s + x'_s \mathcal{E}, \end{aligned} \quad (7)$$

where $\Delta_s = \Delta_a - g_\omega x_s$, $\kappa_s = \kappa_a - g_\kappa x_s$, and $x'_s = \sqrt{2\kappa_a} - g_\kappa x_s / \sqrt{2\kappa_a}$. At the steady state, we have $\dot{\mathcal{O}}_s = 0$,

equivalently

$$\begin{aligned} \omega_m p_s &= 0, \\ g_\omega |a_s|^2 - \omega_m x_s + \frac{ig_\kappa}{\sqrt{2\kappa_a}} (\mathcal{E}^* a_s - \mathcal{E} a_s^*) - \gamma_m p_s &= 0, \\ -(\kappa_s + i\Delta_s) a_s + x'_s \mathcal{E} &= 0. \end{aligned} \quad (8)$$

By solving these equations, we have

$$\begin{aligned} p_s &= 0, \quad a_s = \frac{x'_s \mathcal{E}}{\kappa_s + i\Delta_s}, \\ x_s &= \frac{g_\omega n_s}{\omega_m} + \frac{ig_\kappa}{\sqrt{2\kappa_a}} \cdot \frac{a_s \mathcal{E}^* - a_s^* \mathcal{E}}{\omega_m}. \end{aligned} \quad (9)$$

Obviously, the steady-state displacement of the membrane is determined by both the dispersive and dissipative coupling between photons and phonons. For a *purely dispersive* coupling ($g_\kappa = 0$), x_s is *proportional* to the intracavity mean photon number $n_s = |a_s|^2$ [see the red curve in Fig. 2(a)]. For a *purely dissipative* coupling ($g_\omega = 0$), x_s becomes

$$x_s = [1 - \sqrt{1 - 2(g_\kappa/\kappa_a)^2 (\Delta_a/\omega_m) n_s}] \omega_m \kappa_a, \quad (10)$$

where $x_s \neq 2\kappa_a/g_\kappa$ and $n_s \leq (\kappa_a/g_\kappa)^2 (\omega_m/2\Delta_a)$ are both required. When $n_s = 0$, $x_s = 0$, i.e., the membrane is positioned at its equilibrium. Here x_s and n_s are quadratic dependence for the purely dissipative coupling, demonstrated by the blue curve in Fig. 2(a). One may further notice that the displacement of the membrane caused by the purely dispersive coupling is larger than that caused by the purely dissipative coupling, as clearly shown in Fig. 2(a). To plot Fig. 2(a), we adopt typical experimental parameters [50]: the wavelength of the driving field $\lambda = 1064$ nm, $\omega_d/2\pi = c/\lambda = 281.96$ THz, the quality factor of the membrane $\mathcal{Q}_m = 5.8 \times 10^5$, $\omega_m/2\pi = 136$ kHz, $\gamma_m/2\pi = 0.23$ Hz, $L = 8.7$ cm, $m = 80$ ng, and $\kappa_a/2\pi = 1.5$ MHz. These experimental parameters ensure the stability of the proposed system according to Routh-Hurwitz criterion.

From Eq. (9), one can see that x_s actually satisfies the following cubic equation related to the amplitude of the driving field \mathcal{E} ,

$$ax_s^3 + bx_s^2 + cx_s + d = 0, \quad (11)$$

where

$$\begin{aligned} a &= 2(g_\omega^2 + g_\kappa^2) \omega_m \kappa_a, \\ b &= -4\omega_m \kappa_a (g_\omega \Delta_a + g_\kappa \kappa_a) - 3g_\omega g_\kappa |\mathcal{E}|^2, \\ c &= 2\omega_m \kappa_a (\kappa_a^2 + \Delta_a^2) + 2g_\kappa |\mathcal{E}|^2 (g_\kappa \Delta_a + 4g_\omega \kappa_a), \\ d &= -4\kappa_a |\mathcal{E}|^2 (g_\omega \kappa_a + g_\kappa \Delta_a). \end{aligned} \quad (12)$$

Explicitly, Eq. (11) may have three real roots, corresponding to bistability. But in fact, the bistability can only be predicted for purely dispersive coupling, as shown by the red curve in Fig. 2(b). This indicates that the purely dissipative coupling can not generate the typical stability in optomechanics, demonstrated by the blue curve in Fig. 2(b).

IV. COVARIANCE MATRIX

With steady-state values in hand, we further expand each operator \mathcal{O} around its steady state, i.e., $\mathcal{O} = \delta\mathcal{O} + \mathcal{O}_s$. Substituting this expression back into Eq. (5), we then obtain a set of equations for fluctuations ($\delta\mathcal{O}$). For the strong driving field ($|a_s|^2 \gg 1$), the higher-order fluctuation terms can be safely neglected [28], corresponding to linearization. As a result, the dynamics for fluctuations can be written as

$$\begin{aligned} \dot{\delta x} &= \omega_m \delta p, \\ \dot{\delta p} &= \frac{G_\omega \delta a^\dagger + G_\omega^* \delta a}{\sqrt{2}} - \omega_m \delta x - \gamma_m \delta p + \xi \\ &\quad + \frac{i g_\kappa (\mathcal{E}^* \delta a - \mathcal{E} \delta a^\dagger)}{\sqrt{2\kappa_a}} + \frac{i(G_\kappa \delta a_{\text{in}}^\dagger - G_\kappa^* \delta a_{\text{in}})}{2\sqrt{\kappa_a}}, \quad (13) \\ \dot{\delta a} &= -(\kappa_s + i\Delta_s) \delta a + \left(\frac{G_\kappa + iG_\omega}{\sqrt{2}} - \frac{g_\kappa \mathcal{E}}{\sqrt{2\kappa_a}} \right) \delta x + x'_s a_{\text{in}}, \end{aligned}$$

where $G_{\omega(\kappa)} = \sqrt{2}g_{\omega(\kappa)}a_s$ is the linearized dispersive (dissipative) coupling strength, enhanced by the amplitude of the driving field. By further defining

$$\begin{aligned} \delta x_a &= \frac{\delta a^\dagger + \delta a}{\sqrt{2}}, & \delta p_a &= i \frac{\delta a^\dagger - \delta a}{\sqrt{2}}, \\ x_{\text{in}} &= \frac{a_{\text{in}}^\dagger + a_{\text{in}}}{\sqrt{2}}, & p_{\text{in}} &= i \frac{a_{\text{in}}^\dagger - a_{\text{in}}}{\sqrt{2}}, \end{aligned} \quad (14)$$

Eq. (13) can be rewritten in a more compact form, i.e.,

$$\dot{u}(t) = Au(t) + n(t), \quad (15)$$

where $u^T(t) = (\delta x, \delta p, \delta x_a, \delta p_a)$ is the vector of fluctuation operators, $n(t)$ is the vector of noise operator, given by $n^T(t) = (0, \xi + \frac{G_\kappa}{\sqrt{2\kappa_a}} p_{\text{in}}, x'_s x_{\text{in}}, x'_s p_{\text{in}})$, and the drift matrix A is

$$A = \begin{pmatrix} 0 & \omega_m & 0 & 0 \\ -\omega_m & -\gamma_m & G_\omega + \frac{G_\kappa \Delta_s}{\sqrt{2\kappa_a} x'_s} & -\frac{G_\kappa \kappa_s}{\sqrt{2\kappa_a} x'_s} \\ G_\kappa - \frac{2G_\kappa \kappa_s}{\sqrt{2\kappa_a} x'_s} & 0 & -\kappa_s & \Delta_s \\ G_\omega - \frac{2G_\kappa \Delta_s}{\sqrt{2\kappa_a} x'_s} & 0 & -\Delta_s & -\kappa_s \end{pmatrix}. \quad (16)$$

To obtain the drift matrix A , we have taken a_s as real number, which can be realized by setting $\tan \theta = \Delta_a / \kappa_a$ in Eq. (9).

Since the phonon noise ξ and the photon noise a_{in} are zero-mean quantum Gaussian noises and the dynamics is linearized [see Eq. (13)], the quantum steady state for fluctuations is a zero-mean bipartite Gaussian state, fully described by a 4×4 correlation matrix V , where $V_{ij} = \langle u_i(t) u_j(t') + u_j(t') u_i(t) \rangle / 2$ with $i, j = 1, 2, 3, 4$. The V is obtained by solving the Lyapunov equation $AV + VA^T = -D$, where D is the diffusion matrix, defined by $\langle n_i(t) n_j(t') + n_j(t') n_i(t) \rangle / 2 = D_{ij} \delta(t - t')$. More

specifically, D can be expressed as

$$D = \begin{pmatrix} 0 & 0 & 0 & 0 \\ 0 & \gamma_m(2n_{\text{th}} + 1) + \frac{G_\kappa^2}{4\kappa_a} & 0 & \frac{G_\kappa}{\sqrt{2\kappa_a}} \frac{x'_s}{2} \\ 0 & 0 & \frac{x_s'^2}{2} & 0 \\ 0 & \frac{G_\kappa}{\sqrt{2\kappa_a}} \frac{x'_s}{2} & 0 & \frac{x_s'^2}{2} \end{pmatrix}. \quad (17)$$

Compared to the case of purely dispersive coupling, the dissipative coupling strength appears in the off-diagonal elements of the diffusion matrix, rendering D non-diagonal.

To measure optomechanical entanglement, the logarithmic negativity (E_N) is taken [58], i.e.,

$$E_N \equiv \max[0, -\ln 2\eta^-], \quad (18)$$

where $\eta^- = 2^{-1/2}[\Sigma(V) - (\Sigma(V)^2 - 4\det V)^{1/2}]^{1/2}$ with $\Sigma(V) = \det A + \det B - 2\det C$, $V = \begin{pmatrix} A & C \\ C^T & B \end{pmatrix}$ is the 2×2 block form. When $E_N > 0$ ($= 0$), the state is entangled (separable). Moreover, the larger E_N , the stronger entanglement.

V. OPTOMECHANICAL ENTANGLEMENT

To investigate optomechanical entanglement, we consider three specific scenarios: (i) purely dispersive coupling, (ii) purely dissipative coupling, and (iii) the coexistence of both couplings.

A. Purely dispersive coupling ($g_\kappa = 0$)

In the purely dispersive coupling regime ($g_\kappa = 0$), we present the entanglement measure E_N as a function of both the dispersive coupling strength g_ω and the normalized effective cavity detuning Δ_s / ω_m in Fig. 3(a) to explore the conditions for optimal optomechanical entanglement at a bath temperature of $T = 0.4$ K. The results reveal that the generated entanglement remains relatively weak compared to that typically observed in conventional optomechanical systems. This is primarily due to the inherent limitation in the dispersive coupling strength g_ω (or equivalently G_ω), which must remain small within the stable regime to avoid system instability, thereby restricting the achievable entanglement. Nonetheless, optimal entanglement can still be achieved around the point $(\Delta_s / \omega_m, g_\omega / 2\pi) \approx (2, 3.1)$, as marked by the green star, indicating that even under these constraints, entanglement can be optimized.

To further investigate the role of dispersive coupling strength on entanglement, we plot E_N as a function of g_ω in Fig. 3(b), where $\Delta_s \approx 2\omega_m$ is fixed. It is obviously shown that E_N increases with g_ω . Once up to its maximum, E_N will have a sharp reduction by further increasing g_ω . Such abrupt behavior corresponds to the transition from the stability to instability, as shown by the

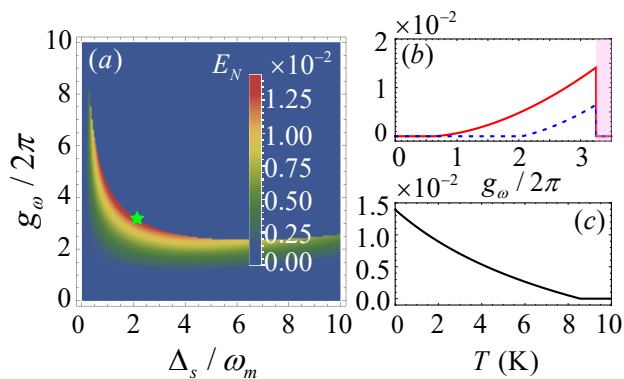


FIG. 3: (a) The logarithmic negativity E_N vs the normalized detuning Δ/ω_m and the purely dispersive coupling strength g_ω at bath temperature $T = 400$ mK. (b) The logarithmic negativity E_N vs the dispersive coupling strength g_ω with $T = 400$ mK (see the red curve) and $T = 4$ K (see the blue dashed curve), where $\Delta_s/\omega_m = 2$ is fixed. (c) The logarithmic negativity E_N vs the bath temperature T with $g_\omega/2\pi = 3.1$ Hz and $\Delta_s/\omega_m = 2$. Other parameters are the same as those in Fig. 2 except for $\mathcal{P} = 50$ mW.

pink-shaded region. Additionally, when the bath temperature increases to $T = 4$ K [see the blue dashed curve], the coupling for generation of quantum entanglement is required to be larger and E_N has a significant reduction. This indicates that quantum entanglement can be affected by the bath temperature. To clearly evaluate the effect of bath temperature, we plot E_N as a function of the bath temperature in Fig. 3(c), where $g_\omega/2\pi = 3.1$ Hz is fixed to obtain optimal entanglement. As the temperature increases, E_N gradually declines. When the bath temperature increases to $T \approx 8.5$ K, $E_N = 0$, that is, quantum entanglement vanishes and the system becomes separable.

B. Purely dissipative coupling ($g_\omega = 0$)

In the purely dissipative case ($g_\omega = 0$), we observe that the optimal entanglement can be significantly stronger than in the purely dispersive case, even surpassing the entanglement achieved in conventional optomechanical systems (i.e., $E_N = 0.35$). This is demonstrated in Fig. 4(a), where E_N is plotted as a function of both the dissipative coupling strength (g_κ) and the normalized effective cavity detuning Δ_s/ω_m . The optimal entanglement is found at approximately $(\Delta_s/\omega_m, g_\kappa/2\pi) \approx (0.1, 20)$, as indicated by the green star. In contrast to the purely dispersive case [see Fig. 2(a)], where the optimal entanglement occurs near the mechanical red sideband at $\Delta_s/\omega_m = 2$, the optimal entanglement in the purely dissipative case is obtained when the cavity is nearly resonant with the driving field, specifically at $\Delta_s/\omega_m = 0.1$, which is far removed from the mechanical red sideband.

Furthermore, in Fig. 4(b), we investigate the behavior of the optomechanical entanglement as a function of the

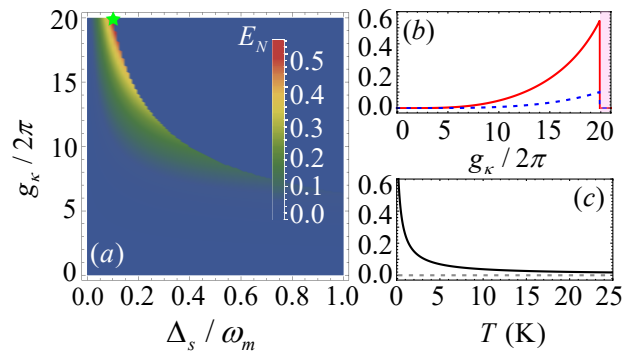


FIG. 4: (a) The logarithmic negativity E_N vs the normalized detuning Δ/ω_m and the purely dissipative coupling strength g_κ at bath temperature $T = 400$ mK. (b) The logarithmic negativity E_N vs the dissipative coupling strength g_κ with $T = 400$ mK (see the red curve) and $T = 4$ K (see the blue dashed curve), where $\Delta_s/\omega_m = 0.1$ is fixed. (c) The logarithmic negativity E_N vs the bath temperature T with $g_\kappa/2\pi = 19$ Hz and $\Delta_s/\omega_m = 0.1$. Other parameters are the same as those in Fig. 2 except for $\mathcal{P} = 50$ mW.

dissipative coupling strength, while fixing $\Delta_s = 0.1\omega_m$. The resulting behavior of E_N mirrors that observed in the purely dispersive case (see the red curve). The abrupt drop in entanglement marks the transition of the system from a stable to an unstable region, as indicated by the pink area. Notably, a relatively large dissipative coupling strength is required to achieve the optimal entanglement. This suggests that in the regime dominated by dissipative coupling, stronger interactions are necessary to generate significant quantum effects. As the bath temperature increases, for instance to $T = 4$ K, the entanglement is reduced (see the blue curve). To explore the influence of bath temperature on optomechanical entanglement, we fix $g_\kappa/2\pi = 19$ Hz and present the results in Fig. 4(c). We observe a sharp decrease in entanglement as the system temperature increases from 0 K to 5 K. However, beyond this point, the entanglement becomes more tolerant to further temperature increases, suggesting that the dissipative coupling becomes more robust to thermal noise at higher temperatures. Remarkably, entanglement persists even up to 25 K. This indicates that strong, noise-resistant entanglement can be generated through purely dissipative coupling, opening new possibilities for quantum information processing and communication in noisy

C. Combined coupling ($g_\omega \neq 0$ and $g_\kappa \neq 0$)

To examine the interplay between dispersive and dissipative coupling effects on optomechanical entanglement, we set the dispersive coupling strength to $g_\omega/2\pi = 3$ Hz, corresponding to the optimal entanglement condition at $\Delta_s/\omega_m = 2$ in the purely dispersive coupling regime [refer to Fig. 3(a)]. By progressively increasing

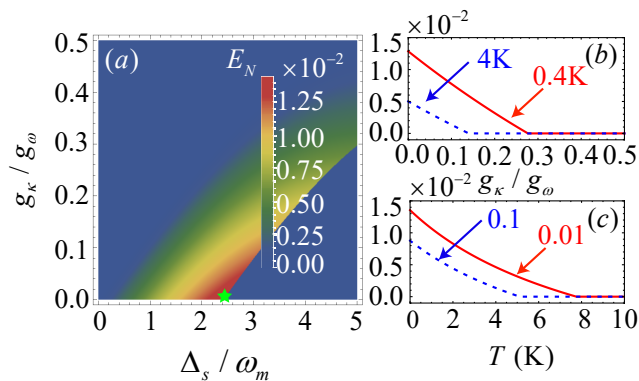


FIG. 5: (a) The logarithmic negativity E_N vs the normalized detuning Δ_s/ω_m and the ratio of g_κ/g_ω at bath temperature $T = 400$ mK. (b) The logarithmic negativity E_N vs the ratio of g_κ/g_ω with $T = 400$ mK (see the red curve) and $T = 4$ K (see the blue dashed curve), where $\Delta_s/\omega_m = 2.2$ is fixed. (c) The logarithmic negativity E_N vs the bath temperature T with $g_\kappa/g_\omega = 0.01$ (see the red curve) and $g_\kappa/g_\omega = 0.1$ K (see the blue dashed curve), where $\Delta_s/\omega_m = 2.2$. Other parameters are the same as those in Fig. 2 except for $\mathcal{P} = 50$ mW, $g_\omega/2\pi = 3$ Hz.

the dissipative coupling strength, we observe a gradual decline in the entanglement, as shown in Fig. 5(a). The reduction in entanglement possibly arises from the interference between the dispersive and dissipative couplings. When the bath temperature increases to $T = 4$ K, it is observed that the optomechanical entanglement is further suppressed, as depicted by the blue dashed curve in Fig. 5(b). Moreover, the larger g_κ is not beneficial to entanglement generation. This can also be revealed by Fig. 5(c), where $g_\kappa/g_\omega = 0.01$ (the red curve) and $g_\kappa/g_\omega = 0.1$ (the blue curve) are taken. For $g_\kappa/g_\omega = 0.1$, the survival temperature of the entanglement is about 5 K. But for $g_\kappa/g_\omega = 0.01$, the survival temperature can

be up to 8 K.

VI. CONCLUSION

In this paper, we investigate quantum entanglement in a dissipative optomechanical system, acted by a fixed mirror and a Michelson–Sagnac interferometer with a membrane. This system allows the dissipative and dispersive couplings to be independently tuned on and off by adjusting the membrane position or the reflectivity (transmissivity) of the beam splitter, enabling us to explore quantum entanglement in three distinct scenarios: purely dispersive case, purely dissipative case, and combined coupling case. Our analysis reveals that, in the purely dispersive case, the steady-state mechanical displacement exhibits a nonlinear dependence on the driving power, whereas in the purely dissipative case, the displacement shows a linear dependence. Furthermore, entanglement generated through purely dissipative coupling is not only significantly stronger but also more noise-tolerant compared to that achieved via purely dispersive coupling. When both coupling mechanisms coexist, quantum entanglement is reduced, likely due to the interference between the two coupling interactions. These findings suggest the potential of purely dissipative coupling to engineer strong and noise-tolerant quantum entanglement, offering a promising pathway for advancing quantum technologies.

This work is supported by the National Natural Science Foundation of China (Grant No. 12175001), the “Pioneer” and “Leading Goose” R&D Program of Zhejiang (Grant No. 2025C01028), the Natural Science Foundation of Zhejiang Province (Grant No. LY24A040004), and the Shenzhen International Quantum Academy (Grant No. SIQA202412).

-
- [1] B. P. Abbott, R. Abbott, T. Abbott, M. Abernathy, F. Acernese, K. Ackley, C. Adams, T. Adams, P. Addesso, R. X. Adhikari, et al., *Phys. Rev. Lett.* **116**, 061102 (2016).
- [2] S. Haroche, *Physics today* **51**, 36 (1998).
- [3] M. Aspelmeyer, T. J. Kippenberg, and F. Marquardt, *Reviews of Modern Physics* **86**, 1391 (2014).
- [4] Y.-C. Liu, Y.-F. Xiao, X. Luan, and C. W. Wong, *Phys. Rev. Lett.* **110**, 153606 (2013).
- [5] J. D. Teufel, T. Donner, D. Li, J. W. Harlow, M. Allman, K. Cicak, A. J. Sirois, J. D. Whittaker, K. W. Lehnert, and R. W. Simmonds, *Nature* **475**, 359 (2011).
- [6] S. Gröblacher, J. B. Hertzberg, M. R. Vanner, G. D. Cole, S. Gigan, K. Schwab, and M. Aspelmeyer, *Nature Physics* **5**, 485 (2009).
- [7] A. Schliesser, R. Rivière, G. Anetsberger, O. Arcizet, and T. J. Kippenberg, *Nature Physics* **4**, 415 (2008).
- [8] X.-Y. Lü, Y. Wu, J. R. Johansson, H. Jing, J. Zhang, and F. Nori, *Phys. Rev. Lett.* **114**, 093602 (2015).
- [9] A. H. Safavi-Naeini, S. Gröblacher, J. T. Hill, J. Chan, M. Aspelmeyer, and O. Painter, *Nature* **500**, 185 (2013).
- [10] T. P. Purdy, P.-L. Yu, R. W. Peterson, N. S. Kampel, and C. A. Regal, *Phys. Rev. X* **3**, 031012 (2013).
- [11] S. Weis, R. Rivière, S. Deléglise, E. Gavartin, O. Arcizet, A. Schliesser, and T. J. Kippenberg, *Science* **330**, 1520 (2010).
- [12] A. H. Safavi-Naeini, T. M. Alegre, J. Chan, M. Eichenfield, M. Winger, Q. Lin, J. T. Hill, D. E. Chang, and O. Painter, *Nature* **472**, 69 (2011).
- [13] A. Kronwald and F. Marquardt, *Phys. Rev. Lett.* **111**, 133601 (2013).
- [14] M. Köppenhöfer, C. Padgett, J. V. Cady, V. Dharod, H. Oh, A. C. Bleszynski Jayich, and A. A. Clerk, *Phys. Rev. Lett.* **130**, 093603 (2023).
- [15] X. Guo, C.-L. Zou, H. Jung, and H. X. Tang, *Phys. Rev. Lett.* **117**, 123902 (2016).

- [16] O. Kyriienko, T. C. H. Liew, and I. A. Shelykh, *Phys. Rev. Lett.* **112**, 076402 (2014).
- [17] W. Xiong, D.-Y. Jin, Y. Qiu, C.-H. Lam, and J. Q. You, *Phys. Rev. A* **93**, 023844 (2016).
- [18] W. Xiong, J. Chen, B. Fang, M. Wang, L. Ye, and J. Q. You, *Phys. Rev. B* **103**, 174106 (2021).
- [19] J. Chen, Z. Li, X.-Q. Luo, W. Xiong, M. Wang, and H.-C. Li, *Opt. Express* **29**, 32639 (2021).
- [20] X.-Y. Lü, W.-M. Zhang, S. Ashhab, Y. Wu, and F. Nori, *Sci Rep* **3**, 2943 (2013).
- [21] M.-L. Peng, M. Tian, X.-C. Chen, G.-Q. Zhang, H.-C. Li, and W. Xiong, arXiv preprint arXiv:2304.13553 (2023).
- [22] W. Xiong, M. Wang, G.-Q. Zhang, and J. Chen, *Phys. Rev. A* **107**, 033516 (2023).
- [23] B. Wang, F. Nori, and Z.-L. Xiang, *Phys. Rev. Lett.* **132**, 053601 (2024).
- [24] N. Mann, M. R. Bakhtiari, A. Pelster, and M. Thorwart, *Phys. Rev. Lett.* **120**, 063605 (2018).
- [25] S. B. Jäger, J. Cooper, M. J. Holland, and G. Morigi, *Phys. Rev. Lett.* **123**, 053601 (2019).
- [26] W. Xiong, Z. Li, Y. Song, J. Chen, G.-Q. Zhang, and M. Wang, *Phys. Rev. A* **104**, 063508 (2021).
- [27] W. Xiong, Z. Li, G.-Q. Zhang, M. Wang, H.-C. Li, X.-Q. Luo, and J. Chen, *Phys. Rev. A* **106**, 033518 (2022).
- [28] D. Vitali, S. Gigan, A. Ferreira, H. Böhm, P. Tombesi, A. Guerreiro, V. Vedral, A. Zeilinger, and M. Aspelmeyer, *Phys. Rev. Lett.* **98**, 030405 (2007).
- [29] L. Tian, *Phys. Rev. Lett.* **108**, 153604 (2012).
- [30] L. Tian, *Phys. Rev. Lett.* **110**, 233602 (2013).
- [31] Y.-D. Wang and A. A. Clerk, *Phys. Rev. Lett.* **110**, 253601 (2013).
- [32] J. Chen, X.-G. Fan, W. Xiong, D. Wang, and L. Ye, *Phys. Rev. A* **109**, 043512 (2024).
- [33] J. Chen, X.-G. Fan, W. Xiong, D. Wang, and L. Ye, *Phys. Rev. B* **108**, 024105 (2023).
- [34] M.-Y. Liu, X.-X. Huang, and W. Xiong (2024), 2404.15111.
- [35] D.-G. Lai, J.-Q. Liao, A. Miranowicz, and F. Nori, *Phys. Rev. Lett.* **129**, 063602 (2022).
- [36] Y.-F. Jiao, S.-D. Zhang, Y.-L. Zhang, A. Miranowicz, L.-M. Kuang, and H. Jing, *Phys. Rev. Lett.* **125**, 143605 (2020).
- [37] Y.-F. Jiao, J.-X. Liu, Y. Li, R. Yang, L.-M. Kuang, and H. Jing, *Phys. Rev. Applied* **18**, 064008 (2022).
- [38] M.-Y. Liu, Y. Gong, J. Chen, Y.-W. Wang, and W. Xiong, arXiv preprint arXiv:2412.20030 (2024).
- [39] C. Ockeloen-Korppi, E. Damskäg, J.-M. Pirkkalainen, M. Asjad, A. Clerk, F. Massel, M. Woolley, and M. Silanpää, *Nature* **556**, 478 (2018).
- [40] F. Elste, S. Girvin, and A. Clerk, *Phys. Rev. Lett.* **102**, 207209 (2009).
- [41] A. Xuereb, R. Schnabel, and K. Hammerer, *Phys. Rev. Lett.* **107**, 213604 (2011).
- [42] O. Kyriienko, T. C. H. Liew, and I. A. Shelykh, *Phys. Rev. Lett.* **112**, 076402 (2014).
- [43] K. Qu and G. Agarwal, *Phys. Rev. A* **91**, 063815 (2015).
- [44] S. Huang and A. Chen, *Phys. Rev. A* **98**, 063818 (2018).
- [45] Y. Liu, Y. Liu, C.-S. Hu, Y.-K. Jiang, H. Wu, and Y. Li, *Phys. Rev. A* **108**, 023503 (2023).
- [46] S. Huang and G. Agarwal, *Phys. Rev. A* **95**, 023844 (2017).
- [47] J. Huang, Y. Li, L. K. Chin, H. Cai, Y. Gu, M. F. Karim, J. Wu, T. Chen, Z. Yang, Y. Hao, et al., *Applied Physics Lett.* **112** (2018).
- [48] T. Kuang, R. Huang, W. Xiong, Y. Zuo, X. Han, F. Nori, C.-W. Qiu, H. Luo, H. Jing, and G. Xiao, *Nature Physics* **19**, 414 (2023).
- [49] Q. Zhang, C. Yang, J. Sheng, and H. Wu, *Proceedings of the National Academy of Sciences* **119**, e2207543119 (2022).
- [50] A. Sawadsky, H. Kaufer, R. M. Nia, S. P. Tarabrin, F. Y. Khalili, K. Hammerer, and R. Schnabel, *Phys. Rev. Lett.* **114**, 043601 (2015).
- [51] D. Friedrich, H. Kaufer, T. Westphal, K. Yamamoto, A. Sawadsky, F. Y. Khalili, S. Danilishin, S. Gößler, K. Danzmann, and R. Schnabel, *New Journal of Physics* **13**, 093017 (2011).
- [52] M. Li, W. H. Pernice, and H. X. Tang, *Phys. Rev. Lett.* **103**, 223901 (2009).
- [53] M. Wu, A. C. Hryciw, C. Healey, D. P. Lake, H. Jayakumar, M. R. Freeman, J. P. Davis, and P. E. Barclay, *Phys. Rev. X* **4**, 021052 (2014).
- [54] R. M. Cole, G. A. Brawley, V. P. Adiga, R. De Alba, J. M. Parpia, B. Ilic, H. G. Craighead, and W. P. Bowen, *Phys. Rev. Applied* **3**, 024004 (2015).
- [55] D. F. Walls and G. Milburn, *Quantum optics* (Springer, Berlin, 1994).
- [56] V. Giovannetti and D. Vitali, *Phys. Rev. A* **63**, 023812 (2001).
- [57] R. Benguria and M. Kac, *Phys. Rev. Lett.* **46**, 1 (1981).
- [58] G. Adesso, A. Serafini, and F. Illuminati, *Phys. Rev. A* **70**, 022318 (2004).